Imagined Autocurricula

Ahmet H. Güzel* University College London AI Centre Matthew T. Jackson University of Oxford

Jarek L. Liesen University of Oxford **Tim Rocktäschel** University College London AI Centre **Jakob N. Foerster** University of Oxford

Ilija Bogunovic University College London AI Centre Jack Parker-Holder
University College London AI Centre

Abstract

Training agents to act in embodied environments typically requires vast training data or access to accurate simulation, neither of which exists for many cases in the real world. Instead, *world models* are emerging as an alternative–leveraging offline, passively collected data, they make it possible to generate diverse worlds for training agents in simulation. In this work, we harness world models to generate "imagined" environments to train robust agents capable of generalizing to novel task variations. One of the challenges in doing this is ensuring the agent trains on *useful* generated data. We thus propose a novel approach IMAC (Imagined Autocurricula) leveraging Unsupervised Environment Design (UED), which induces an automatic curriculum over generated worlds. In a series of challenging, procedurally generated environments, we show it is possible to achieve strong transfer performance on held-out environments having trained only inside a world model learned from a narrower dataset. We believe this opens the path to utilizing larger-scale, foundation world models for generally capable agents.

1 Introduction

Despite significant advancements in AI, we remain far from generally capable agents [1]. In the 2010s, progress towards this goal was driven by breakthroughs in deep reinforcement learning (RL, [2]) where agents such as AlphaGo [3] showed it was possible to discover new knowledge beyond human capabilities, like the famous *move37*. However, scaling RL in simulation to produce a more general intelligence remains bottlenecked by the lack of sufficiently diverse and real-world simulators [4, 5]. By contrast, more recent years have been dominated by agents trained from vast quantities of Internet data. Here, agents have a broader knowledge of the real world but lack of ability to discover new, superhuman behaviors since they are largely trained to mimic the training data.

World models are emerging as a promising approach to leverage the best of both. They "stand on the shoulders of giants" by training on vast Internet data [6, 7, 8, 9, 10], but then enable agents to train with RL inside their generated (or *imagined*) environments. Thus, world models make it possible for agents to imagine potential outcomes without direct environment interaction, allowing them to train across diverse scenarios with substantially fewer real experiences [11, 12, 13, 14, 15, 16, 17]. In theory, large foundation world models could then be used to generate sufficiently rich environments for agents to learn superhuman behaviors for a swathe of embodied settings. Progress in world models research has typically fallen into two categories.

^{*}Corresponding author (ahmet.guzel.23@ucl.ac.uk).

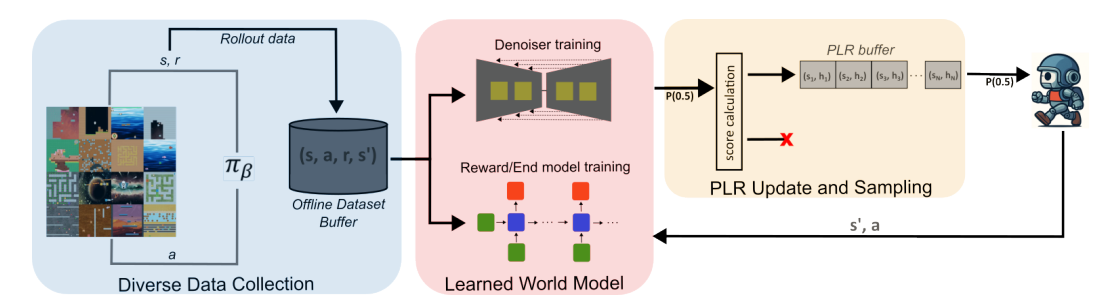


Figure 1: Architecture overview: (1) Offline Data Collection: Diverse state-action-reward-next state tuples are collected via policy π_{β} to form the dataset. (2) World Model Training: A state transition denoiser and reward/termination predictor are trained on the dataset and frozen for consistency. (3) Agent Training: The agent learns through an imagine-based autocurriculum using Prioritized Level Replay, which balances between sampling from existing experiences and generating new rollouts to update the buffer.

The first seeks to train world models from single (online or offline) environments, achieving strong and sample-efficient performance [18, 19, 17]. The latter sees more general, so-called foundation world models trained from large-scale internet data [6, 7, 9, 10], but these models have not been shown to be useful for training generalist agents.

In this paper, we attempt to bridge this gap. We focus on the offline RL setting, where agents must learn from pre-collected datasets without additional environment interaction [20]. We focus on procedurally generated environments, meaning our offline data contains sequences (action labelled videos) from a variety of different levels. We then seek to transfer the learned agents to new, unseen levels from the same environment. This presents a significant challenge for existing methods, which often fail to generalize to new tasks when training purely from offline data [21, 22]. We believe world models can be the solution to this problem-we first train a diffusion world model from the offline samples and then use it to generate new, imagined worlds. Crucially, naively generating data from world models can lead to ineffective training data, making agent learning inefficient. This inefficiency stems from both the quality of the worlds themselves and the challenge of setting appropriate hyperparameters like imagined episode length across diverse tasks. To address this challenge, we leverage the Unsupervised Environment Design paradigm (UED) [23])—where a teacher proposes levels that maximize student regret. Rather than training on fixed or random sets of imagined worlds, we create an Imagined Autocurricula, or IMAC. Importantly, our framework is world-model agnostic—while we use a diffusion world model as our foundation, our autocurriculum approach can be applied to any world model architecture that provides reward and next-token predictions. Our contribution lies not in advancing world model architectures, but in demonstrating how UED principles can effectively guide agent training within learned world models from offline mixed dataset.

Our approach IMAC uses Prioritized Level Replay (PLR, [24]) as a UED algorithm, which we show provides a natural complement to the learned world model—the world model generates diverse potential training trajectories or "imagined environments," while PLR strategically selects subsequent training tasks from these imagined rollouts. Figure 1 illustrates the overall architecture of our approach. As we show, this prioritization process naturally induces an automatic curriculum over the generated, imagined worlds, meaning the agent is exposed to increasingly challenging training tasks. As a testbed for this paradigm, we leverage seven Procgen environments with high-dimensional visual inputs, where both model-free [25] and model-based approaches [26] struggle to transfer knowledge to unseen scenarios [21, 22]. The resulting agents have significantly stronger generalization performance than state-of-the-art baselines, demonstrating strong transfer performance on held-out environments having trained only inside a world model learned from a narrower dataset. We believe this opens the path to utilizing larger-scale, foundation world models for generally capable agents.

Our primary contribution is the demonstration that world models offer the path to training on diverse offline datasets and subsequently generalizing to new, unseen tasks. Importantly, this is made possible by training on an Imagined Autocurriculum; rather than fixing hyperparameters or randomizing settings, each of which could be problematic for learning. We believe this is the first example of open-ended learning in learned world models, and could enable significant progress towards generalist agents with ever more powerful world models in the future.

2 Preliminaries

2.1 (Offline) Reinforcement Learning

To model environments, we consider Partially Observable Markov Decision Processes (POMDPs) [2], which are defined by a tuple $\langle S, A, T, R, \Omega, O, \gamma \rangle$. S, A, and Ω respectively represent the set of states, actions, and observations. $T(s_{t+1}|a_t,s_t)$ is the conditional transition distribution over the next state $s_{t+1} \in S$ given previous action $a_t \in A$ and state $s_t \in S$. Each transition produces an observation $o_{t+1} \in \Omega$ sampled from $O(o_{t+1}|s_{t+1},a_t)$, and a reward $r_{t+1} \in \mathbb{R}$ sampled from $R(r_{t+1}|s_{t+1},a_t,s_t)$.

An agent interacting with the POMDP observes o_t and maintains a belief state b_t based on the history of observations and actions. The agent then selects an action a_t according to its policy. Reinforcement learning aims to find the optimal policy — a conditional distribution $\pi(a_t|h_t)$ that maximizes the expected discounted return $\mathbb{E}\left[\sum_{t=0}^{\infty} \gamma^t r_t\right]$, where r_t is the reward received at time step t, $\gamma \in [0,1)$ is the discount factor, and h_t represents the history of observations and actions up to time t. In offline reinforcement learning, the agent cannot interact directly with the POMDP, but is given a dataset \mathcal{D} of previously recorded interactions $(o_t, a_t, r_{t+1}, o_{t+1})$. There are no restrictions on how \mathcal{D} is collected, so it may include data from a mix of policies with varying levels of expertise and state space coverage. Generalizing to states that differ from those in \mathcal{D} is the main challenge of offline RL.

2.2 World Models

A world model [27] is a parameterized model of an environment that can be used to train reinforcement learning agents and autoregressively generate synthetic data. World models are able to generate imaginary trajectories by sampling from the following joint distribution:

$$p(s_{t+1:T}, r_{t+1:T}, a_{t:T-1}|s_t) = \prod_{i=t}^{T-1} \pi(a_i|s_i) T(s_{i+1}|s_i, a_i) R(r_{i+1}|s_i, a_i).$$
 (1)

Creating a world model for a POMDP requires modeling the transition and observation distributions T and O, and reward distribution R. Given a dataset \mathcal{D} of interactions, we optimize the model parameters to minimize an expected loss

$$\min_{\hat{T},\hat{O},\hat{R}} \mathbb{E}_r \left[L_O(\hat{o}_t, o_t) + L_R(\hat{r}_t, r_t) \right], \tag{2}$$

where \hat{o}_t and \hat{r}_t are the world model predictions of o_t and r_t given a_t, o_{t-1} , and L_O, L_R are appropriate loss functions. In practice, instead of predicting the next observation based on the prediction for the next state, we can predict it directly from the previous observation and action buffer, learning state transition dynamics implicitly via a hidden state (e.g., that of a recurrent neural network). Additionally, it is common to predict the residual in the observation $\Delta \hat{o}_{t+1} = \hat{o}_{t+1} - o_t$, which biases the world model towards temporal consistency in the autoregressive prediction.

2.3 Diffusion Models

Inspired by non-equilibrium thermodynamics, diffusion models [28] generate data by reversing a gradual noising process. The forward process corrupts a data sample $\mathbf{x}_0 \sim q(\mathbf{x}_0)$ into pure Gaussian noise $\mathbf{x}_T \sim \mathcal{N}(\mathbf{0}, \mathbf{I})$ through a Markov chain of Gaussian transitions:

$$q(\mathbf{x}_t \mid \mathbf{x}_{t-1}) = \mathcal{N}(\mathbf{x}_t; \sqrt{1 - \beta_t} \, \mathbf{x}_{t-1}, \beta_t \mathbf{I}), \tag{3}$$

where $\{\beta_t\}_{t=1}^T$ is a fixed variance schedule. The generative model learns the reverse process $p_{\theta}(\mathbf{x}_{t-1} \mid \mathbf{x}_t)$ by approximating the *score function*, i.e., the gradient of the log posterior $\nabla_{\mathbf{x}_t} \log q(\mathbf{x}_t \mid \mathbf{x}_0)$. In practice, a neural network $\epsilon_{\theta}(\mathbf{x}_t, t)$ is trained to predict the noise added during the forward process, and the training objective is typically:

$$\mathcal{L}_{\text{simple}} = \mathbb{E}_{\mathbf{x}_{0}, t, \epsilon} \left[\left\| \epsilon - \epsilon_{\theta}(\mathbf{x}_{t}, t) \right\|^{2} \right], \tag{4}$$

where
$$\epsilon \sim \mathcal{N}(\mathbf{0}, \mathbf{I})$$
 and $\mathbf{x}_t = \sqrt{\bar{\alpha}_t} \, \mathbf{x}_0 + \sqrt{1 - \bar{\alpha}_t} \, \epsilon$ with $\bar{\alpha}_t = \prod_{s=1}^t (1 - \beta_s)$.

This score matching framework, introduced by [29], enables estimation of score models directly from empirical data without requiring explicit knowledge of the true underlying score function. While standard diffusion models typically function as unconditional generators of a data distribution $p_{\rm data}(x)$, adapting them for sequential decision-making requires conditioning on past information to predict future states.

To employ diffusion models as world models, we extend ϵ_{θ} to model the environment's dynamics $p(x_{t+1}|x_{\leq t},a_{\leq t})$, where x_{t+1} is the next observation, while $x_{\leq t}$ and $a_{\leq t}$ denote the history of past observations and actions. This adaptation is particularly relevant for POMDPs, where the true environmental state must be inferred from observation and action sequences. The modified score model ϵ_{θ} is trained by extending the standard diffusion objective to:

$$L(\theta) = \mathbb{E} \left\| \epsilon_{\theta}(x_{\tau}^{t+1}, \tau, x_{0}^{\leq t}, a^{\leq t}) - \epsilon \right\|^{2}$$
 (5)

where x_{τ}^{t+1} is the noised version of the next observation at noise level τ , and ϵ is the noise added during the forward process.

To generate a subsequent observation x_{t+1} , we iteratively solve the reverse-time Stochastic Differential Equation (SDE)—or an equivalent Ordinary Differential Equation (ODE)—guided by our history-conditioned score model. While various numerical solvers can be employed, there exists a practical trade-off: sample quality typically improves with increased Number of Function Evaluations (NFE), directly impacting the computational cost of the diffusion-based world model during inference.

2.4 Prioritized Level Replay

When training agents to solve procedurally generated environments, previous methods have commonly relied on continuously and uniformly sampling new levels during training. This can be sample-inefficient since many sampled levels do not contribute significantly to the agent's learning progress. As an alternative, Prioritized Level Replay (PLR) [24] has been proposed, where levels are replayed based on their potential to induce greater learning progress in the agent. In original PLR implementation, it maintains a buffer of previously encountered levels, including a score that represents an estimate of learning potential and a staleness factor that represents how long ago that level was sampled. There are many possible choices for computing the score — a simple yet effective one is given by the TD-error $\delta_t = r_t + V(s_{t+1}) - V(s_t)$. During training, we randomly select between sampling a randomly generated level with a selected episode length range randomly and sampling one from the buffer. When sampling from the buffer, a level l_i is selected for replay with probability

$$l_i \sim (1 - \rho) \cdot P_S(l \mid \Lambda_{\text{seen}}, S) + \rho \cdot P_C(l \mid \Lambda_{\text{seen}}, C, c), \tag{6}$$

which is a mixture distribution of P_S and P_C with parameter ρ . They prioritize levels with high scores and high staleness, respectively. Here $\Lambda_{\rm seen}$ is the replay buffer, S is the level scores, C is the last time each level was sampled, and c is how many levels were sampled since the beginning of training. In our world model setting, we save both the initial state s_0 and the desired imagination horizon h in the buffer. When the algorithm samples an entry from the buffer, it uses the same initial state s_0 to begin imagination and runs the world model forward for exactly h steps. By interpreting world models as procedural generators of agent experience, we can directly apply PLR to prioritize the most valuable imagined experiences. This yields a novel method for model-based offline RL that efficiently leverages imagined trajectories.

3 Imagined Autocurricula

Our approach consists of three key components: (1) a diffusion world model trained from diverse offline data, (2) using this model to generate imagined random episode length rollouts for agent training, and (3) implementing an auto curriculum over these imagined environments.

3.1 Diffusion World Model Training

First, we collect a diverse visual offline dataset of different behaviors (expert, medium, and random) via behavior policy as $D = \{(o_i, a_i, r_i, o_i')\}_{i=1}^N$. Then we train the diffusion model as a conditional

generative model of environment dynamics, $p(x_{t+1}|x_{< t}, a_{< t})$, handling the POMDP setting where the true Markovian state is unknown and must be approximated from history. Our training objective follows Equation 5. Following DIAMOND [11], we utilize the Elucidating Diffusion Models (EDM) formulation [30] rather than the traditional DDPM [28] approach. This critical design choice enables our world model to remain stable over long time horizons with significantly fewer denoising steps. During training, we sample trajectory segments from our dataset and apply noise using a τ -level perturbation kernel to create training pairs. To incorporate temporal context, we maintain a buffer containing L=4 previous observations and actions as conditioning information. Our diffusion world model implements a standard 2D U-Net architecture [31] as the core denoising network. The temporal information flows through two pathways: past observations are concatenated channelwise with the noisy observation being denoised, while action information is integrated via adaptive group normalization layers [32] within residual blocks [33]. We iteratively solve the reverse SDE using Euler's method with exactly 5 denoising steps. We also follow their approach of using fullimage observations (64×64 3-channel for Procgen) rather than discrete latent space representations, as they demonstrated superior performance over other state-of-the-art world models that use discrete latent space. Given the similar image dimensions between Atari and our Procgen environment, we leveraged their extensively validated hyperparameter settings for our diffusion model. Their comprehensive ablation study showed these parameters achieve both notable image generation quality and computational efficiency, making them an ideal foundation for our work. This approach allows our diffusion model to capture fine visual details critical for reinforcement learning for Procgen agents, such as small rewards and enemies, while maintaining temporal consistency across long sequences.

3.2 Agent Training in Imagined Environments

With our diffusion world model trained, we implement auxiliary predictors for reward and termination signals using an ensemble of E prediction heads to capture uncertainty during imagined rollouts. While the base architecture follows Alonso et al. [11], employing a separate model R_{ψ} with standard CNN [34] and LSTM [35] layers to handle partial observability, we extend their approach through our ensemble of prediction heads, which provides crucial uncertainty estimates during long-horizon planning in our POMDP setting. This model is trained on the same offline dataset used for the world model, optimizing for accurate reward and episode termination predictions, with the agent using the mean of the ensemble predictions during training. Building upon these diffusion and auxiliary models, the RL agent follows an actor-critic architecture parameterized by a shared CNN-LSTM backbone with separate policy and value function heads. The agent is trained using Advantage Actor-Critic (A2C) [36] with λ -returns for advantage estimation as in [37]. The policy head π_{ϕ} is optimized to maximize expected returns while the value network V_{ϕ} minimizes the temporal difference error between predicted values and the computed λ -returns.

During training, we generate imagined trajectories by first sampling an initial state s_0 from our diverse offline dataset, then autoregressively producing sequences of states, rewards, and termination signals by rolling out our policy through the diffusion denoiser model and ensemble auxiliary predictors. Unlike the fixed horizon approach in [11], we randomly sample the imagined episode length between minimum and maximum horizon bounds to incorporate greater diversity in training experiences and prevent the agent from exploiting fixed-horizon dynamics. Finally, we compute policy gradients and value updates based on these imagined experiences, enabling effective policy learning without additional environment interaction.

3.3 Autocurriculum

Our IMAC implementation follows the PLR framework [24], maintaining a replay buffer of previously encountered initial states s_0 with associated priority scores. For each training iteration, with probability 0.5, we train the agent using the current policy and world model on initial states sampled from this prioritized buffer. With the remaining 0.5 probability, we select a random initial state and a random imagined episode length, T, to explore the environment space and update the buffer. The priority score for each initial state s_0 is computed using the agent's temporal difference errors, δ_k , which serve as a proxy for learning potential. The specific formula for the score is:

$$score(s_0) = \frac{1}{T} \sum_{t=0}^{T} \sum_{k=t}^{T} (\gamma \lambda)^{k-t} \max(0, \delta_k).$$
 (7)

Here, T is the length of the imagined episode (which is randomly chosen during the exploration phase), δ_k is the temporal difference error at timestep k, γ is the discount factor, and λ is the trace decay parameter. The inner sum, $\sum_{k=t}^{T} (\gamma \lambda)^{k-t} \max(0, \delta_k)$, represents a truncated, discounted, and λ -weighted sum of future *positive* TD errors from timestep t to T. We specifically focus on positive TD errors through the $\max(0, \delta_k)$ operation because they indicate instances where the agent's value estimate was too low, suggesting unexpectedly good outcomes that are particularly valuable for learning. The outer sum and division by T average this sum over all timesteps t in the episode. Based on this prioritization mechanism, we believe that our approach creates three key advantages for generalization: First, by focusing on the scenarios with the highest learning potential, the agent spends more computation on informative experiences rather than those where little can be learned. Second, the random horizon setting creates diversity in training experiences, preventing the agent from exploiting fixed-length dynamics. Finally, the prioritization mechanism naturally discovers an emergent curriculum that gradually increases in difficulty as the agent improves. The emergent curriculum effect is particularly important for procedurally generated environments, where the difficulty distribution can be complex and unknown a priori. Our IMAC approach discovers this difficult landscape dynamically during training, focusing on the boundary of the agent's current capabilities—what PLR authors call "threshold levels" that provide the highest learning signal. As the agent improves, this boundary shifts to more challenging scenarios, creating a curriculum that scales with the agent's abilities without requiring manual design or environment-specific knowledge. Importantly, unlike previous autocurriculum learning approaches that require direct control of the environment generation process, our method works entirely within the imagined random-length rollouts from our world model, which we call our imagined autocurricula, making it applicable to any environment where a world model can be trained, including those where the procedural generation process is a black box. Details of model architecture, algorithm, training hyperparameters used, and dataset details for this work are given in Appendices A and B, C, and D.

4 Experiments

4.1 Procgen Benchmark

For comprehensive evaluation of our approach, we use a challenging subset of the Procgen Benchmark [38], a collection of procedurally generated environments designed specifically to test generalization in reinforcement learning. Unlike the Atari benchmark used in previous world model studies [11, 16, 15, 17, 39], Procgen environments are procedurally generated and thus inherently test an agent's ability to generalize to unseen levels with the same underlying mechanics.

We created a mixed offline dataset capturing diverse interaction patterns to represent the type of diverse data we may see in Internet videos. Similar to "mixed" datasets in existing benchmarks [40, 22] it consists of three complementary components: Expert trajectories ($D_{\rm expert}$) from fully trained PPO agents, Medium-quality trajectories ($D_{\rm medium}$) from partially trained agents reaching approximately 50% of expert performance, and Random exploration trajectories ($D_{\rm random}$) to ensure broad state space coverage. This mixture forms a dataset $D = D_{\rm random} \cup D_{\rm expert} \cup D_{\rm medium}$ totaling 1 million transitions per game across 200 training levels. We focus on seven environments from Procgen: CoinRun, Ninja, Jumper, Maze, and CaveFlyer, selected based on their poor performance in previous offline RL benchmarks [21] and their sparse reward structure. For each environment, we use 200 levels for training our world model while evaluating generalization on unseen test levels (201- ∞). After data collection, we trained the world model and reward/termination predictors (requiring approximately 10 hours on an NVIDIA RTX 4090), then froze these components for generating imagined rollouts during agent training. Each agent seed's training required approximately 4 days on a single RTX 4090, with experiments conducted across 3 random seeds for 5 million total steps each, resulting in 180 GPU days of computation.

We compare our approach with several established offline RL methods including Behavior Cloning (BC), Conservative Q-Learning (CQL) [41], Implicit Q-Learning (IQL) [42], Batch-Constrained Q-learning (BCQ) [43], Behavior-Constrained Transformers (BCT), and Decision Transformers (DT) [44]. We also conducted an ablation study comparing our approach against world model baselines, evaluating the impact of both fixed (15 steps) and variable (between 5 and 22 steps) imagined episode lengths.

4.2 Procgen Benchmark Results

Table 1: **Generalization results**: All values represent the mean return over three random seeds \pm standard deviation when transferring agents to held out levels on the Procgen benchmark.

							-
Method	CoinRun	Ninja	Jumper	Maze	CaveFlyer	Heist	Miner
BC	5.31 ± 0.31	4.22 ± 0.21	3.92 ± 0.42	4.03 ± 0.29	3.12 ± 0.17	2.1 ± 0.22	4.68 ± 0.11
CQL	5.12 ± 0.22	3.29 ± 0.32	2.24 ± 0.31	1.82 ± 0.12	1.89 ± 0.27	0.3 ± 0.09	0.32 ± 0.09
IQL	4.96 ± 0.20	3.11 ± 0.31	2.35 ± 0.38	1.98 ± 0.17	1.45 ± 0.47	0.27 ± 0.04	0.5 ± 0.08
BCQ	4.33 ± 0.14	3.14 ± 0.26	2.29 ± 0.18	1.83 ± 0.14	2.21 ± 0.61	0.44 ± 0.12	0.42 ± 0.13
BCT	5.11 ± 0.10	4.33 ± 0.28	3.72 ± 0.37	3.98 ± 0.19	2.76 ± 0.22	1.5 ± 0.23	1.08 ± 0.10
DT	5.03 ± 0.18	4.03 ± 0.31	3.84 ± 0.24	4.32 ± 0.11	3.04 ± 0.32	1.82 ± 0.09	1.11 ± 0.09
iMac	6.20 ± 0.14	5.15 ± 0.12	5.78 ± 0.21	5.41 ± 0.19	$\textbf{3.87} \pm 0.22$	2.91 ± 0.15	5.61 ± 0.13

Table 2: **World model ablation**: Performance evaluation on the Procgen benchmark all values represent mean return over three random seeds ± standard deviation

Method	CoinRun	Ninja	Jumper	Maze	CaveFlyer	Heist	Miner
WM Fixed	4.76 ± 0.19	3.78 ± 0.21	3.71 ± 0.19	3.92 ± 0.32	2.94 ± 0.13	2.05 ± 0.14	3.18 ± 0.10
WM Random	5.36 ± 0.15	4.33 ± 0.18	4.11 ± 0.11	4.62 ± 0.15	3.02 ± 0.19	2.19 ± 0.18	4.55 ± 0.15
iMac	6.20 ± 0.14	$\textbf{5.15} \pm 0.12$	$\textbf{5.78} \pm 0.21$	$\textbf{5.41} \pm 0.19$	$\textbf{3.87} \pm 0.22$	$\textbf{2.91} \pm 0.15$	5.61 ± 0.13

The results in Table 1 demonstrate that IMAC method consistently outperforms state-of-the-art of-fline RL algorithms across all evaluated Procgen environments. Our approach achieves improvements of 17% on CoinRun, 19% on Ninja, 48% on Jumper, 35% on Maze, 24% on CaveFlyer, 38% on Heist, and 19% on Miner compared to the best-performing model-free baseline for each environment.

Table 2 further demonstrates IMAC's effectiveness through ablation studies comparing different horizon-setting strategies. While both fixed and random episode length world model approaches show strong performance, our IMAC method incorporating prioritized initial state selection consistently delivers improved results—achieving up to 56% improvement over the fixed horizon baseline on Jumper and 38% on Maze. These results provide compelling evidence that procedural generalization in world models benefits significantly from our autocurriculum approach, which automatically discovers and focuses training on the most informative scenarios. The substantial performance advantage across diverse environments demonstrates that IMAC effectively addresses the core challenge of generalization from limited offline datasets in procedurally generated environments. We provide all the hyperparameters used in model-free baseline algorithms in Appendix F.

To provide a comprehensive statistical analysis of our approach's effectiveness, Figure 2 presents the aggregated mean performance improvements across all evaluated environments, offering quantitative evidence of the consistent generalization benefits achieved by our method compared to the baselines presented in both tables.

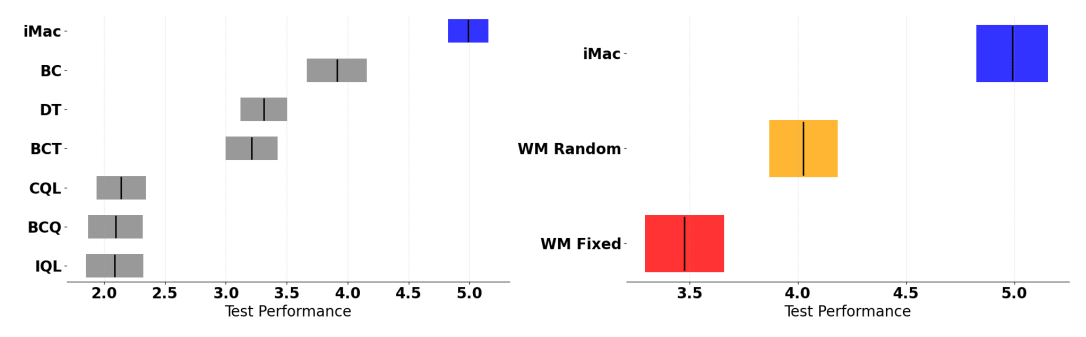


Figure 2: Mean test performance across seven Procgen environments. Left: Comparison of modelfree baselines against our proposed IMAC method. Right: World model ablation study comparing WM variants (Fixed and Random) against the full iMac approach

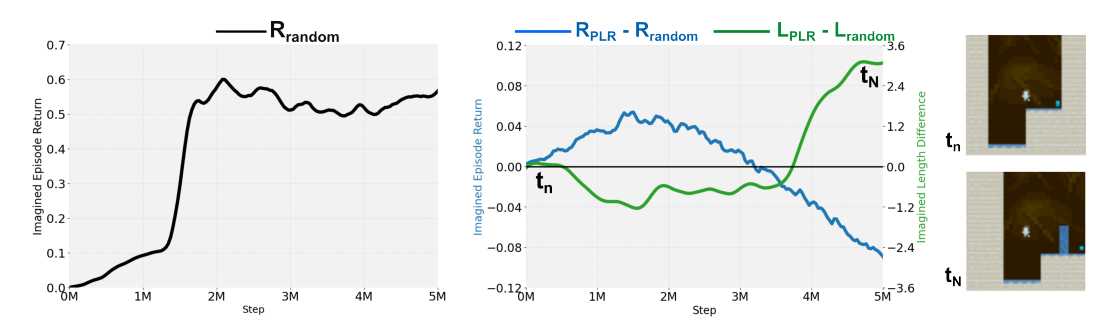


Figure 3: Evolution of performance and episode length during training with our Imagined Autocurricula approach. **Left:** Mean episodic return of the random baseline (R_{Random}) showing steady improvement over training steps. **Right:** The difference between PLR and Random approaches in terms of both return ($R_{PLR} - R_{Random}$) and imagined episode length ($L_{PLR} - L_{Random}$).

Our results provide compelling evidence for the effectiveness of the emergent curriculum created by our Imagined Autocurricula approach. As shown in Figure 3, initially PLR selects similar episode lengths as random sampling while achieving higher returns for CoinRun. However, after approximately 4M steps, a significant shift occurs—PLR begins prioritizing substantially longer episodes while temporarily accepting lower comparative returns. This demonstrates the emergent curriculum effect: our prioritization mechanism automatically discovers and focuses on more challenging, temporally-extended scenarios aps the agent's capabilities improve.

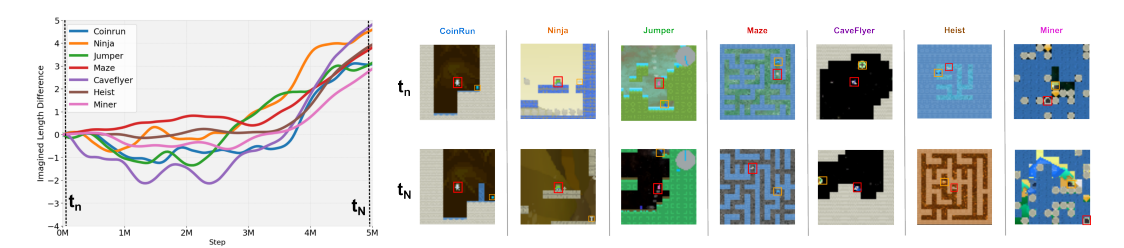


Figure 4: Left: Difference in imagined episode length between PLR and Random baselines across seven Proceen environments. Right: Example frames from early t_n and late t_N training stages, with red boxes representing agents and orange boxes representing rewards.

The visual examples in Figure 4 further illustrate this curriculum effect across all environments. Comparing initial states t_0 with later states t_N , we observe a clear progression in complexity—from simple, direct paths to complex obstacle arrangements for CoinRun, and from straightforward corridors to intricate maze structures requiring extended planning in Maze. The image pairs show representative states from early and late training stages, illustrating the progression from simpler to more complex scenarios. This progressive increase in horizon differences correlates directly with our method's performance on test environments, supporting our hypothesis that learning temporally extended behaviors is crucial for generalization in procedurally generated environments. What's particularly notable is that this curriculum emerges naturally from our prioritization mechanism without any explicit difficulty programming or environment-specific knowledge. Our method discovers this effective learning progression while training exclusively on imagined rollouts from a fixed world model trained on offline data, validating our core claim that prioritizing states based on their learning potential substantially improves generalization capabilities.

5 Related Work

Generalization in Reinforcement Learning has been extensively studied, though primarily in online settings where agents can actively collect new data during training [45, 46, 47, 38, 48, 49, 50, 51, 52, 53, 54, 55, 56, 57, 58, 59]. Benchmarks for evaluating generalization capabilities have evolved from environment suites like Procgen [38] and NetHack [41] for online settings, to more recent offline alternatives such as V-D4RL and OFFLINE PROCGEN [22, 21]. These offline benchmarks

present unique challenges, particularly in visual domains where balancing dataset scale and accessibility becomes crucial—large-scale datasets like Atari, StarCraft, and MineRL contain millions of samples but require substantial computational resources [60, 61, 62], while more accessible alternatives offer 100,000 to 1 million samples per environment. Despite this progress, generalization in offline RL remains relatively unexplored compared to its online counterpart, especially when dealing with procedurally generated environments where model-free methods have shown significant limitations. Our work addresses this gap by leveraging world models to improve generalization across diverse procedurally generated environments without requiring additional environment interaction beyond the initial offline dataset.

World Models have evolved significantly since the first introduction of the concept of reinforcement learning within an imagined neural network environment [27]. Early applications to Atari games through SimPLe [39] established the Atari 100k benchmark, highlighting the sample efficiency benefits of model-based approaches. The field advanced substantially with DreamerV2 [17], which pioneered learning directly from the latent space of a recurrent state space model (RSSM), while DreamerV3 [12] achieved human-level performance across diverse domains using consistent hyperparameters. Recent architectural innovations include transformer-based approaches such as TWM [16] and STORM [32], which adapt DreamerV2's and DreamerV3's RSSM frameworks respectively, employing different tokenization strategies. IRIS [15] represents an alternative approach, constructing a language of image tokens through a discrete autoencoder and composing these tokens temporally using an autoregressive transformer. Most recently, DIAMOND [11] introduced diffusion models as an alternative to discrete latent representations for world modeling, demonstrating that improved visual fidelity can lead to better agent performance, particularly for tasks where fine visual details are critical. Recent advances in video generation, including 3D DiT architectures like CogVideoX [63], Cosmos [9], and realistic world generators like Genie 3 [8] offer promising alternatives for world modeling. While we employ a 2D UNet for computational efficiency, our curriculum learning framework is architecture- agnostic and could leverage these more advanced architectures as they become computationally more feasible. There has also been work using world models to generalize to unseen tasks [64, 65], however these were focused on a domain randomization setting (e.g. our "random" baseline) rather than an automated curriculum. By contrast, our work builds upon these foundations and leverages PLR to generate an emergent curriculum, which subsequently improves generalization to unseen tasks.

Curriculum Learning in RL applies the principle of gradually increasing task difficulty to reinforcement learning, improving both training efficiency and generalization capabilities [66, 67]. Determining learning priorities is central to effective curriculum design, with various measures including reward signals [68], learning progress [69], TD-errors [70], and state novelty [71]. Recent advances in automated curriculum learning [72] have reduced reliance on manual design, with methods like Prioritized Level Replay (PLR) [24] demonstrating that targeting environments with the highest learning potential creates an emergent curriculum that progressively challenges the agent at the frontier of its capabilities. While we employ PLR in our implementation, our framework is compatible with other UED algorithms including ACCEL [73], which uses evolution strategies for curriculum design; ADD [74], which leverages diffusion models for adversarial environment generation. These methods could potentially be integrated into our framework, highlighting the modularity of our approach. Our work applies this curriculum-based approach to world models, creating an imagined autocurriculum that operates entirely within generated rollouts from a fixed world model trained on offline data, enabling effective generalization without requiring explicit environment control or online interaction.

6 Limitations

While our approach demonstrates promising results, we acknowledge certain constraints inherent to offline world modeling. The quality of generated scenarios naturally depends on training data diversity, though our mixed-expertise dataset mitigates this concern in practical settings. Implementation of IMAC requires substantial computational resources, and its effectiveness varies across environment types. Future work could address these limitations through efficiency optimizations, domain-adaptive world modeling techniques, automated parameter tuning, and improved uncertainty quantification. Additional promising directions include innovative data augmentation strategies and extensions to continuous control domains with higher-dimensional state spaces—all building upon our demonstrated foundation. We provide computational cost analysis for our method in Appendix G.

7 Conclusion

We introduced IMAC, a novel approach combining diffusion-based world models with automatic curriculum learning to train general agents. Our method leverages offline data to generate diverse imagined environments and employs Prioritized Level Replay to create an emergent curriculum that adapts to the agent's capabilities. Experimental results across seven Procgen environments demonstrate that IMAC consistently outperforms state-of-the-art offline RL algorithms and world model baselines, achieving improvements of up to 48% compared to model-free approaches and 56% over fixed-horizon world models. The emergent curriculum proves particularly effective for environments requiring extended planning horizons and complex navigation. Our work demonstrates that strong transfer performance on held-out environments is possible using only imagined trajectories from a world model trained on a limited dataset. This finding opens a promising path toward utilizing larger-scale foundation world models for developing generally capable agents that can handle novel task variations.

Future work should address the current limitations of our approach by exploring techniques to reduce computational requirements, investigating novel curriculum learning methodologies with world model architectures with stronger uncertainty quantification, and developing methods to automatically adapt prioritization parameters based on environment characteristics. Additionally, extending IMAC to continuous control domains and environments with higher complexity or extremely sparse rewards represents an important direction for expanding the applicability of our method.

8 Acknowledgements

This work was supported by the Engineering and Physical Sciences Research Council (EPSRC) EP/S021566/1.

References

- [1] Meredith Ringel Morris, Jascha Sohl-dickstein, Noah Fiedel, Tris Warkentin, Allan Dafoe, Aleksandra Faust, Clement Farabet, and Shane Legg. Levels of AGI: Operationalizing Progress on the Path to AGI. In *The International Conference on Machine Learning*, 2024.
- [2] Richard S. Sutton and Andrew G. Barto. *Reinforcement Learning: An Introduction*. The MIT Press, second edition, 2018.
- [3] David Silver, Aja Huang, Chris J. Maddison, Arthur Guez, Laurent Sifre, George van den Driessche, Julian Schrittwieser, Ioannis Antonoglou, Veda Panneershelvam, Marc Lanctot, Sander Dieleman, Dominik Grewe, John Nham, Nal Kalchbrenner, Ilya Sutskever, Timothy Lillicrap, Madeleine Leach, Koray Kavukcuoglu, Thore Graepel, and Demis Hassabis. Mastering the game of Go with deep neural networks and tree search, January 2016.
- [4] Open Ended Learning Team, Adam Stooke, Anuj Mahajan, Catarina Barros, Charlie Deck, Jakob Bauer, Jakub Sygnowski, Maja Trebacz, Max Jaderberg, Michael Mathieu, Nat McAleese, Nathalie Bradley-Schmieg, Nathaniel Wong, Nicolas Porcel, Roberta Raileanu, Steph Hughes-Fitt, Valentin Dalibard, and Wojciech Marian Czarnecki. Open-Ended Learning Leads to Generally Capable Agents, July 2021.
- [5] Adaptive Agent Team, Jakob Bauer, Kate Baumli, Satinder Baveja, Feryal Behbahani, Avishkar Bhoopchand, Nathalie Bradley-Schmieg, Michael Chang, Natalie Clay, Adrian Collister, Vibhavari Dasagi, Lucy Gonzalez, Karol Gregor, Edward Hughes, Sheleem Kashem, Maria Loks-Thompson, Hannah Openshaw, Jack Parker-Holder, Shreya Pathak, Nicolas Perez-Nieves, Nemanja Rakicevic, Tim Rocktäschel, Yannick Schroecker, Jakub Sygnowski, Karl Tuyls, Sarah York, Alexander Zacherl, and Lei Zhang. Human-Timescale Adaptation in an Open-Ended Task Space, January 2023.
- [6] J Parker-Holder, P Ball, J Bruce, V Dasagi, K Holsheimer, C Kaplanis, A Moufarek, G Scully, J Shar, J Shi, et al. Genie 2: A large-scale foundation world model, 2024.

- [7] Jake Bruce, Michael Dennis, Ashley Edwards, Jack Parker-Holder, Yuge Shi, Edward Hughes, Matthew Lai, Aditi Mavalankar, Richie Steigerwald, Chris Apps, Yusuf Aytar, Sarah Bechtle, Feryal Behbahani, Stephanie Chan, Nicolas Heess, Lucy Gonzalez, Simon Osindero, Sherjil Ozair, Scott Reed, Jingwei Zhang, Konrad Zolna, Jeff Clune, Nando de Freitas, Satinder Singh, and Tim Rocktäschel. Genie: Generative Interactive Environments. In *The International Conference on Machine Learning*, 2024.
- [8] Philip J. Ball, Jakob Bauer, Frank Belletti, Bethanie Brownfield, Ariel Ephrat, Shlomi Fruchter, Agrim Gupta, Kristian Holsheimer, Aleksander Holynski, Jiri Hron, Christos Kaplanis, Marjorie Limont, Matt McGill, Yanko Oliveira, Jack Parker-Holder, Frank Perbet, Guy Scully, Jeremy Shar, Stephen Spencer, Omer Tov, Ruben Villegas, Emma Wang, Jessica Yung, Cip Baetu, Jordi Berbel, David Bridson, Jake Bruce, Gavin Buttimore, Sarah Chakera, Bilva Chandra, Paul Collins, Alex Cullum, Bogdan Damoc, Vibha Dasagi, Maxime Gazeau, Charles Gbadamosi, Woohyun Han, Ed Hirst, Ashyana Kachra, Lucie Kerley, Kristian Kjems, Eva Knoepfel, Vika Koriakin, Jessica Lo, Cong Lu, Zeb Mehring, Alex Moufarek, Henna Nandwani, Valeria Oliveira, Fabio Pardo, Jane Park, Andrew Pierson, Ben Poole, Helen Ran, Tim Salimans, Manuel Sanchez, Igor Saprykin, Amy Shen, Sailesh Sidhwani, Duncan Smith, Joe Stanton, Hamish Tomlinson, Dimple Vijaykumar, Luyu Wang, Piers Wingfield, Nat Wong, Keyang Xu, Christopher Yew, Nick Young, Vadim Zubov, Douglas Eck, Dumitru Erhan, Koray Kavukcuoglu, Demis Hassabis, Zoubin Gharamani, Raia Hadsell, Aäron van den Oord, Inbar Mosseri, Adrian Bolton, Satinder Singh, and Tim Rocktäschel. Genie 3: A new frontier for world models. Google Deepmind, 2025.
- [9] NVIDIA, :, Niket Agarwal, Arslan Ali, Maciej Bala, Yogesh Balaji, Erik Barker, Tiffany Cai, Prithvijit Chattopadhyay, Yongxin Chen, Yin Cui, Yifan Ding, Daniel Dworakowski, Jiao-jiao Fan, Michele Fenzi, Francesco Ferroni, Sanja Fidler, Dieter Fox, Songwei Ge, Yunhao Ge, Jinwei Gu, Siddharth Gururani, Ethan He, Jiahui Huang, Jacob Huffman, Pooya Jannaty, Jingyi Jin, Seung Wook Kim, Gergely Klár, Grace Lam, Shiyi Lan, Laura Leal-Taixe, Anqi Li, Zhaoshuo Li, Chen-Hsuan Lin, Tsung-Yi Lin, Huan Ling, Ming-Yu Liu, Xian Liu, Alice Luo, Qianli Ma, Hanzi Mao, Kaichun Mo, Arsalan Mousavian, Seungjun Nah, Sriharsha Niverty, David Page, Despoina Paschalidou, Zeeshan Patel, Lindsey Pavao, Morteza Ramezanali, Fitsum Reda, Xiaowei Ren, Vasanth Rao Naik Sabavat, Ed Schmerling, Stella Shi, Bartosz Stefaniak, Shitao Tang, Lyne Tchapmi, Przemek Tredak, Wei-Cheng Tseng, Jibin Varghese, Hao Wang, Haoxiang Wang, Heng Wang, Ting-Chun Wang, Fangyin Wei, Xinyue Wei, Jay Zhangjie Wu, Jiashu Xu, Wei Yang, Lin Yen-Chen, Xiaohui Zeng, Yu Zeng, Jing Zhang, Qinsheng Zhang, Yuxuan Zhang, Qingqing Zhao, and Artur Zolkowski. Cosmos world foundation model platform for physical ai, 2025.
- [10] Sherry Yang, Yilun Du, Seyed Kamyar Seyed Ghasemipour, Jonathan Tompson, Leslie Pack Kaelbling, Dale Schuurmans, and Pieter Abbeel. Learning interactive real-world simulators. In *The Twelfth International Conference on Learning Representations*, 2024.
- [11] Eloi Alonso, Adam Jelley, Vincent Micheli, Anssi Kanervisto, Amos Storkey, Tim Pearce, and François Fleuret. Diffusion for world modeling: Visual details matter in atari, 2024.
- [12] Danijar Hafner, Jurgis Pasukonis, Jimmy Ba, and Timothy Lillicrap. Mastering diverse domains through world models, 2024.
- [13] Quentin Garrido, Mahmoud Assran, Nicolas Ballas, Adrien Bardes, Laurent Najman, and Yann LeCun. Learning and leveraging world models in visual representation learning, 2024.
- [14] Philipp Wu, Alejandro Escontrela, Danijar Hafner, Ken Goldberg, and Pieter Abbeel. Day-dreamer: World models for physical robot learning, 2022.
- [15] Vincent Micheli, Eloi Alonso, and François Fleuret. Transformers are sample-efficient world models, 2023.
- [16] Jan Robine, Tobias Uelwer, and Stefan Harmeling. Smaller world models for reinforcement learning, 2023.
- [17] Danijar Hafner, Timothy Lillicrap, Mohammad Norouzi, and Jimmy Ba. Mastering atari with discrete world models, 2020.

- [18] Danijar Hafner, Timothy Lillicrap, Ian Fischer, Ruben Villegas, David Ha, Honglak Lee, and James Davidson. Learning latent dynamics for planning from pixels, 2018.
- [19] Danijar Hafner, Timothy Lillicrap, Jimmy Ba, and Mohammad Norouzi. Dream to control: Learning behaviors by latent imagination. In *International Conference on Learning Representations*, 2020.
- [20] Sergey Levine, Aviral Kumar, George Tucker, and Justin Fu. Offline reinforcement learning: Tutorial, review, and perspectives on open problems, 2020.
- [21] Ishita Mediratta, Qingfei You, Minqi Jiang, and Roberta Raileanu. The generalization gap in offline reinforcement learning, 2024.
- [22] Cong Lu, Philip J. Ball, Tim G. J. Rudner, Jack Parker-Holder, Michael A. Osborne, and Yee Whye Teh. Challenges and opportunities in offline reinforcement learning from visual observations, 2023.
- [23] Michael Dennis, Natasha Jaques, Eugene Vinitsky, Alexandre Bayen, Stuart Russell, Andrew Critch, and Sergey Levine. Emergent complexity and zero-shot transfer via unsupervised environment design, 2020.
- [24] Minqi Jiang, Edward Grefenstette, and Tim Rocktäschel. Prioritized level replay. In *International Conference on Machine Learning*, pages 4940–4950. PMLR, 2021.
- [25] Rafael Figueiredo Prudencio, Marcos R. O. A. Maximo, and Esther Luna Colombini. A survey on offline reinforcement learning: Taxonomy, review, and open problems, August 2024.
- [26] Haoyang He. A survey on offline model-based reinforcement learning, 2023.
- [27] David Ha and Jürgen Schmidhuber. World models, 2018.
- [28] Jonathan Ho, Ajay Jain, and Pieter Abbeel. Denoising diffusion probabilistic models, 2020.
- [29] Aapo Hyvärinen. Estimation of non-normalized statistical models by score matching, 2005.
- [30] Tero Karras, Miika Aittala, Timo Aila, and Samuli Laine. Elucidating the design space of diffusion-based generative models, 2022.
- [31] Olaf Ronneberger, Philipp Fischer, and Thomas Brox. U-net: Convolutional networks for biomedical image segmentation, 2015.
- [32] Ruimao Zhang, Zhanglin Peng, Lingyun Wu, Zhen Li, and Ping Luo. Exemplar normalization for learning deep representation, 2020.
- [33] Kaiming He, Xiangyu Zhang, Shaoqing Ren, and Jian Sun. Deep residual learning for image recognition, 2015.
- [34] Y. LeCun, B. Boser, J. S. Denker, D. Henderson, R. E. Howard, W. Hubbard, and L. D. Jackel. Backpropagation applied to handwritten zip code recognition, 1989.
- [35] Sepp Hochreiter and Jürgen Schmidhuber. Long short-term memory, November 1997.
- [36] Volodymyr Mnih, Adrià Puigdomènech Badia, Mehdi Mirza, Alex Graves, Timothy P. Lillicrap, Tim Harley, David Silver, and Koray Kavukcuoglu. Asynchronous methods for deep reinforcement learning, 2016.
- [37] John Schulman, Philipp Moritz, Sergey Levine, Michael Jordan, and Pieter Abbeel. Highdimensional continuous control using generalized advantage estimation, 2015.
- [38] Karl Cobbe, Christopher Hesse, Jacob Hilton, and John Schulman. Leveraging procedural generation to benchmark reinforcement learning, 2020.
- [39] Lukasz Kaiser, Mohammad Babaeizadeh, Piotr Milos, Blazej Osinski, Roy H Campbell, Konrad Czechowski, Dumitru Erhan, Chelsea Finn, Piotr Kozakowski, Sergey Levine, Afroz Mohiuddin, Ryan Sepassi, George Tucker, and Henryk Michalewski. Model-based reinforcement learning for atari, 2024.

- [40] Justin Fu, Aviral Kumar, Ofir Nachum, George Tucker, and Sergey Levine. D4{rl}: Datasets for deep data-driven reinforcement learning, 2021.
- [41] Aviral Kumar, Aurick Zhou, George Tucker, and Sergey Levine. Conservative q-learning for offline reinforcement learning, 2020.
- [42] Ilya Kostrikov, Ashvin Nair, and Sergey Levine. Offline reinforcement learning with implicit q-learning, 2021.
- [43] Scott Fujimoto, David Meger, and Doina Precup. Off-policy deep reinforcement learning without exploration, 2019.
- [44] Lili Chen, Kevin Lu, Aravind Rajeswaran, Kimin Lee, Aditya Grover, Michael Laskin, Pieter Abbeel, Aravind Srinivas, and Igor Mordatch. Decision transformer: Reinforcement learning via sequence modeling, 2021.
- [45] Aravind Rajeswaran, Vikash Kumar, Abhishek Gupta, Giulia Vezzani, John Schulman, Emanuel Todorov, and Sergey Levine. Learning complex dexterous manipulation with deep reinforcement learning and demonstrations, 2018.
- [46] Marlos C. Machado, Marc G. Bellemare, Erik Talvitie, Joel Veness, Matthew Hausknecht, and Michael Bowling. Revisiting the arcade learning environment: Evaluation protocols and open problems for general agents, 2017.
- [47] Charles Packer, Katelyn Gao, Jernej Kos, Philipp Krähenbühl, Vladlen Koltun, and Dawn Song. Assessing generalization in deep reinforcement learning, 2019.
- [48] Robert Kirk, Amy Zhang, Edward Grefenstette, and Tim Rocktäschel. A survey of zero-shot generalisation in deep reinforcement learning, 2023.
- [49] Niels Justesen, Ruben Rodriguez Torrado, Philip Bontrager, Ahmed Khalifa, Julian Togelius, and Sebastian Risi. Illuminating generalization in deep reinforcement learning through procedural level generation, 2018.
- [50] Alex Nichol, Vicki Pfau, Christopher Hesse, Oleg Klimov, and John Schulman. Gotta learn fast: A new benchmark for generalization in rl, 2018.
- [51] Heinrich Küttler, Nantas Nardelli, Alexander H. Miller, Roberta Raileanu, Marco Selvatici, Edward Grefenstette, and Tim Rocktäschel. The nethack learning environment, 2020.
- [52] Emmanuel Bengio, Joelle Pineau, and Doina Precup. Interference and generalization in temporal difference learning, 2020.
- [53] Martin Bertran, Natalia Martinez, Mariano Phielipp, and Guillermo Sapiro. Instance based generalization in reinforcement learning, 2020.
- [54] Dibya Ghosh, Jad Rahme, Aviral Kumar, Amy Zhang, Ryan P Adams, and Sergey Levine. Why generalization in rl is difficult: Epistemic pomdps and implicit partial observability. In M. Ranzato, A. Beygelzimer, Y. Dauphin, P.S. Liang, and J. Wortman Vaughan, editors, Advances in Neural Information Processing Systems, volume 34, pages 25502–25515. Curran Associates, Inc., 2021.
- [55] Jiafei Lyu, Le Wan, Xiu Li, and Zongqing Lu. Understanding what affects generalization gap in visual reinforcement learning: Theory and empirical evidence, 2024.
- [56] Andy Ehrenberg, Robert Kirk, Minqi Jiang, Edward Grefenstette, and Tim Rocktäschel. A study of off-policy learning in environments with procedural content generation. In *ICLR Workshop on Agent Learning in Open-Endedness*, 2022.
- [57] Clare Lyle, Mark Rowland, Will Dabney, Marta Kwiatkowska, and Yarin Gal. Learning dynamics and generalization in reinforcement learning, 2022.
- [58] Mhairi Dunion, Trevor McInroe, Kevin Sebastian Luck, Josiah Hanna, and Stefano V. Albrecht. Conditional mutual information for disentangled representations in reinforcement learning. In *Conference on Neural Information Processing Systems*, 2023.

- [59] Abdulaziz Almuzairee, Nicklas Hansen, and Henrik I. Christensen. A recipe for unbounded data augmentation in visual reinforcement learning, 2024.
- [60] Rishabh Agarwal, Dale Schuurmans, and Mohammad Norouzi. An optimistic perspective on offline reinforcement learning, 2020.
- [61] Oriol Vinyals, Timo Ewalds, Sergey Bartunov, Petko Georgiev, Alexander Sasha Vezhnevets, Michelle Yeo, Alireza Makhzani, Heinrich Küttler, John Agapiou, Julian Schrittwieser, John Quan, Stephen Gaffney, Stig Petersen, Karen Simonyan, Tom Schaul, Hado van Hasselt, David Silver, Timothy Lillicrap, Kevin Calderone, Paul Keet, Anthony Brunasso, David Lawrence, Anders Ekermo, Jacob Repp, and Rodney Tsing. Starcraft ii: A new challenge for reinforcement learning, 2017.
- [62] Linxi Fan, Guanzhi Wang, Yunfan Jiang, Ajay Mandlekar, Yuncong Yang, Haoyi Zhu, Andrew Tang, De-An Huang, Yuke Zhu, and Anima Anandkumar. Minedojo: Building open-ended embodied agents with internet-scale knowledge, 2022.
- [63] Zhuoyi Yang, Jiayan Teng, Wendi Zheng, Ming Ding, Shiyu Huang, Jiazheng Xu, Yuanming Yang, Wenyi Hong, Xiaohan Zhang, Guanyu Feng, Da Yin, Yuxuan Zhang, Weihan Wang, Yean Cheng, Bin Xu, Xiaotao Gu, Yuxiao Dong, and Jie Tang. Cogvideox: Text-to-video diffusion models with an expert transformer, 2025.
- [64] Philip J Ball, Cong Lu, Jack Parker-Holder, and Stephen Roberts. Augmented world models facilitate zero-shot dynamics generalization from a single offline environment. In Marina Meila and Tong Zhang, editors, *Proceedings of the 38th International Conference on Machine Learning*, volume 139 of *Proceedings of Machine Learning Research*, pages 619–629. PMLR, 18–24 Jul 2021.
- [65] Kimin Lee, Younggyo Seo, Seunghyun Lee, Honglak Lee, and Jinwoo Shin. Context-aware dynamics model for generalization in model-based reinforcement learning. In *International Conference on Machine Learning*, 2020.
- [66] Yoshua Bengio, Jérôme Louradour, Ronan Collobert, and Jason Weston. Curriculum learning. In *International Conference on Machine Learning*, 2009.
- [67] Tambet Matiisen, Avital Oliver, Taco Cohen, and John Schulman. Teacher-student curriculum learning, 2017.
- [68] Marcin Andrychowicz, Filip Wolski, Alex Ray, Jonas Schneider, Rachel Fong, Peter Welinder, Bob McGrew, Josh Tobin, Pieter Abbeel, and Wojciech Zaremba. Hindsight experience replay, 2018.
- [69] Rémy Portelas, Cédric Colas, Katja Hofmann, and Pierre-Yves Oudeyer. Teacher algorithms for curriculum learning of deep rl in continuously parameterized environments. In Leslie Pack Kaelbling, Danica Kragic, and Komei Sugiura, editors, *Proceedings of the Conference on Robot Learning*, volume 100 of *Proceedings of Machine Learning Research*, pages 835–853. PMLR, 30 Oct–01 Nov 2020.
- [70] Tom Schaul, John Quan, Ioannis Antonoglou, and David Silver. Prioritized experience replay, 2016.
- [71] Nikolay Savinov, Anton Raichuk, Raphaël Marinier, Damien Vincent, Marc Pollefeys, Timothy Lillicrap, and Sylvain Gelly. Episodic curiosity through reachability, 2019.
- [72] Alex Graves, Marc G. Bellemare, Jacob Menick, Remi Munos, and Koray Kavukcuoglu. Automated curriculum learning for neural networks, 2017.
- [73] Jack Parker-Holder, Minqi Jiang, Michael Dennis, Mikayel Samvelyan, Jakob Foerster, Edward Grefenstette, and Tim Rocktäschel. Evolving curricula with regret-based environment design, 2023.
- [74] Hojun Chung, Junseo Lee, Minsoo Kim, Dohyeong Kim, and Songhwai Oh. Adversarial environment design via regret-guided diffusion models, 2024.

- [75] Steven Kapturowski, Georg Ostrovski, John Quan, Remi Munos, and Will Dabney. Recurrent experience replay in distributed reinforcement learning, 05 2019.
- [76] Yuxin Wu and Kaiming He. Group normalization, 2018.
- [77] Stefan Elfwing, Eiji Uchibe, and Kenji Doya. Sigmoid-weighted linear units for neural network function approximation in reinforcement learning, 2017.

NeurIPS Paper Checklist

1. Claims

Ouestion: Do the main claims made in the abstract and introduction accurately reflect the paper's contributions and scope?

Answer: [Yes]

Justification: The contributions outlined in the introduction are fully demonstrated through our experimental results.

2. Limitations

Question: Does the paper discuss the limitations of the work performed by the authors?

Answer: [Yes]

Justification: Limitations of our work are discussed in Section 6.

3. Theory Assumptions and Proofs

Question: For each theoretical result, does the paper provide the full set of assumptions and a complete (and correct) proof?

Answer: [NA]

Justification: The paper contains no theoretical results.

4. Experimental Result Reproducibility

Question: Does the paper fully disclose all the information needed to reproduce the main experimental results of the paper to the extent that it affects the main claims and/or conclusions of the paper (regardless of whether the code and data are provided or not)?

Answer: [Yes]

Justification: Our introduced domain is fully detailed in Section 3, while all hyperparameters used are provided in the Supplemantary Material.

5. Open access to data and code

Question: Does the paper provide open access to the data and code, with sufficient instructions to faithfully reproduce the main experimental results, as described in supplemental material?

Answer: [Yes]

Justification: The pipeline uses already open-sourced codebases, and the remainder of the code will be released on GitHub shortly after this submission.

6. Experimental Setting/Details

Ouestion: Does the paper specify all the training and test details (e.g., data splits, hyperparameters, how they were chosen, type of optimizer, etc.) necessary to understand the results?

Answer: [Yes]

Justification: This information partly stated in the experiments section and full details are included in the supplementary material.

7. Experiment Statistical Significance

Question: Does the paper report error bars suitably and correctly defined or other appropriate information about the statistical significance of the experiments?

Answer: [Yes]

Justification: All results are run over multiple seeds with error bars reported.

8. Experiments Compute Resources

Question: For each experiment, does the paper provide sufficient information on the computer resources (type of compute workers, memory, time of execution) needed to reproduce the experiments?

Answer: [Yes]

A Model Architectures

Diffusion World Model The diffusion model D_{θ} employs a standard 2D U-Net architecture [31] for next-frame prediction. The model conditions on a history window of 4 previous frames and their corresponding actions, along with the diffusion timestep τ . We implement observation conditioning through frame stacking along the channel dimension, while action and diffusion time conditioning are incorporated via adaptive group normalization layers [32] within the U-Net's residual blocks.

Reward and Termination Predictor The reward/termination model R_{ψ} utilizes a shared backbone architecture with separate prediction heads for reward and termination signals. Crucially, we employ an ensemble of 10 prediction heads to enable uncertainty quantification during imagination rollouts. The model processes sequences of frames and actions through convolutional residual blocks [33] followed by an LSTM cell [36, 35]. During inference, the ensemble predictions are aggregated to compute both mean estimates and uncertainty measures, providing robustness against prediction errors in long-horizon imagined trajectories. Prior to imagination, we perform burn-in [75] using the conditioning frames and actions to properly initialize the LSTM's hidden and cell states.

Actor-Critic Network The policy π_{ϕ} and value network V_{ϕ} share a common feature extraction backbone with separate output layers. We refer to this combined architecture as the actor-critic network $(\pi,V)_{\phi}$, though technically V represents a state-value function rather than an action-value critic. The network processes individual frames through a convolutional encoder consisting of four residual blocks with 2×2 max-pooling (stride 2) between blocks. Each residual block contains a main path with group normalization [76], SiLU activation [77], and 3×3 convolution (stride 1, padding 1). The convolutional features are then processed by an LSTM cell to maintain temporal context. Similar to the reward model, we initialize the LSTM states through burn-in on conditioning frames before beginning the imagination procedure.

Please refer to Table 3 below for hyperparameter values.

Table 3: Architecture Parameters for iMAC.

Hyperparameter	Value
Diffusion Model (D_{θ})	
Observation conditioning mechanism	Frame stacking
Action conditioning mechanism	Adaptive Group Normalization
Diffusion time conditioning mechanism	Adaptive Group Normalization
Residual blocks layers	[2, 2, 2, 2]
Residual blocks channels	[64, 64, 64, 64]
Residual blocks conditioning dimension	256
Reward/Termination Model (R_{ψ})	
Action conditioning mechanism	Adaptive Group Normalization
Residual blocks layers	[2, 2, 2, 2]
Residual blocks channels	[32, 32, 32, 32]
Residual blocks conditioning dimension	128
LSTM dimension	512
Actor-Critic Model (π_{ϕ} and V_{ϕ})	
Residual blocks layers	[1, 1, 1, 1]
Residual blocks channels	[32, 32, 64, 64]
LSTM dimension	512

B World Model Training Parameters

Table 4: Hyperparameters for IMAC.

Table 4: Hyperparameters for IMAC	
Hyperparameter	Value
Training loop	
Number of epochs	1000
Training steps per epoch	100
Batch size	32
Environment steps per epoch	100
Epsilon (greedy) for collection	0.01
RL hyperparameters	
Imagination horizon (H)	Fixed:15, Random:[5-22]
Discount factor (γ)	0.985
Entropy weight (η)	0.001
λ -returns coefficient (λ)	0.95
Sequence construction during training	
For D_{θ} , number of conditioning observations and actions (L)	4
For R_{ψ} , burn-in length (B_R) , set to L in practice	4
For R_{ψ} , training sequence length $(B_R + H)$	Fixed:19, Random[9-26]
For π_{ϕ} and V_{ϕ} , burn-in length $(B_{\pi,V})$, set to L in practice	4
	·
Optimization	A J XV
Optimizer	AdamW
Learning rate	4e-5
Epsilon	1e-8
Weight decay (D_{θ})	1e-2
Weight decay (R_{ψ})	1e-2
Weight decay $(\pi_{\phi} \text{ and } V_{\phi})$	5e-5
Diffusion Sampling	
Method	Euler
Number of steps	5
Environment	
Image observation dimensions	$64 \times 64 \times 3$
Action space	Discrete (up to 18 actions)
Frameskip	4
Max noop	30
Termination on life loss	True
Reward clipping	$\{0,1\}$
PLR	
Stalaness Factor	0.1
Buffer Size	2500
•	· ·

C Baseline World Model and Actor-Critic Training Algorithm

Algorithm 1: iMac (Sequential Offline Training) **Procedure** training loop(D)// D is a fixed offline dataset: **Phase 1: Train Diffusion Model:** for epochs_diffusion do do for steps diffusion model do do $update_diffusion_model(D);$ end end // Freeze Diffusion Model D_{θ} ; Phase 2: Train Reward/Termination Model; for epochs_reward do do for steps reward end model do do update_reward_end_model(D); end end // Freeze Reward/Termination Model R_{ψ} ; Phase 3: Train Actor-Critic with Frozen Models; for epochs_actor_critic do do for steps actor critic do do update actor critic(D); // Uses frozen D_{θ} and R_{ψ} end end **Procedure** $update_diffusion_model(D)$ Sample sequence $(x_{t-L+1}^0, a_{t-L+1}, \dots, x_t^0, a_t, x_{t+1}^0) \sim D;$ Sample $\log(\sigma) \sim \mathcal{N}(F_{mean}, F_{std}^2)$ // \log -normal sigma distribution from EDM; Define $\tau := \sigma$ // default identity schedule from EDM; Sample $x_{t+1}^1 \sim \mathcal{N}(x_{t+1}^0, \sigma^2 I)$ // Add independent Gaussian noise; Compute $x_{t+1}^0 = D_{\theta}(x_{t+1}^1, \tau, x_{t-L+1}^0, a_{t-L+1}, \dots, x_t^0, a_t)$; Compute reconstruction loss $\mathcal{L}(\theta) = ||x_{t+1}^0 - x_{t+1}^1||^2$; Update D_{θ} ; **Procedure** update reward end model(D) Sample indices $I := \{t, \dots, t + L + H - 1\}$ // burn-in + imagination horizon; Sample sequence $(x_i^0, a_i, r_i, d_i)_{i \in I} \sim D$; Initialize h = c = 0 // LSTM hidden and cell states; for $i \in I$ do do Compute \hat{r}_i , \hat{d}_i , h, $c = R_{\psi}(x_i, a_i, h, c)$; Compute $\mathcal{L}(\psi) = \sum_{i \in I} \text{CE}(r_i, \text{sign}(r_i)) + \text{CE}(d_i, \hat{d}_i) \text{ // CE: cross-entropy loss;}$ Update R_{ψ} ; **Procedure** update_actor_critic(D) Sample initial buffer $(x_{t-L+1}^0, a_{t-L+1}, \dots, x_t^0) \sim D;$ Burn-in buffer with R_{ψ} , π_{ϕ} and V_{ϕ} to initialize LSTM states; for i = t to t + H - 1 do do

Algorithm 2: iMac: Actor-Critic Training with PLR (Prioritized Level Replay)

```
Procedure train\_actor\_critic\_PLR(D, B)
    //D is the offline dataset, B is the prioritized buffer;
    for epochs_actor_critic do do
         // Update buffer with probability 0.5;
         if random() < 0.5 then then
             update PLR buffer(D, B);
         end
         for steps_actor_critic do do
              // Train actor-critic using only buffer data;
              update actor critic from buffer(B);
         end
    end
Procedure update PLR buffer(D, B)
    // Sample horizon length randomly;
    Sample initial sequence (x_{t-L+1}^0, a_{t-L+1}, \dots, x_t^0) \sim D;
Burn-in buffer with R_{\psi}, \pi_{\phi} and V_{\phi} to initialize LSTM states;
    // Imagine trajectory using frozen models;
    Initialize trajectory \tau = \{\};
    for i = t to t + H - 1 do do
         Sample a_i \sim \pi_{\phi}(a_i|x_i^0);
         Sample reward r_i and termination d_i with frozen R_{\psi};
         Sample next observation x_{i+1}^0 by simulating reverse diffusion process with frozen D_{\theta};
         Compute TD-error \delta_i = r_i + \gamma V_{\phi}(x_{i+1}^0) - V_{\phi}(x_i^0);
         \tau \leftarrow \tau \cup \{(x_i^0, a_i, r_i, d_i, x_{i+1}^0, \delta_i)\};
         if d_i = 1 then then
             break;
         end
    end
    // Calculate PLR score as positive mean TD-error;
    Compute PLR score s_{\tau} = \text{mean}(\max(\delta_i, 0) \text{ for } \delta_i \text{ in } \tau);
    // Update buffer if score is higher than any existing entry;
    if s_{\tau} > \min(s_b \text{ for } b \in B) then then
        Replace lowest-scoring entry in B with (\tau, s_{\tau});
    end
Procedure update\_actor\_critic\_from\_buffer(B)
    // Sample trajectory from buffer based on priorities;
    Sample trajectory \tau \sim B according to PLR scores;
    // Extract states, actions, rewards, etc.;
    Extract (x_i^0, a_i, r_i, d_i, x_{i+1}^0) from \tau;
    // Compute values for all states in trajectory;
    Compute V_{\phi}(x_i^0) for all states in \tau;
    // Compute advantage estimates and returns;
    Compute advantages A_i and returns G_i for all transitions;
    // Update actor and critic;
    Compute RL losses \mathcal{L}_V(\phi) = \sum_i (V_\phi(x_i^0) - G_i)^2;
Compute \mathcal{L}_\pi(\phi) = -\sum_i \log \pi_\phi(a_i|x_i^0) \cdot A_i;
    Update \pi_{\phi} and V_{\phi};
```

D Dataset Collection Details

We constructed our offline dataset by collecting trajectories from 200 procedurally generated levels for each of the five Procgen environments (CoinRun, Ninja, Jumper, Maze, and CaveFlyer), totaling 1 million environment steps per game. We explicitly constrained data collection to levels 0-199 for each environment, ensuring complete isolation from the test levels (200+) used for evaluation, thereby preventing any potential data leakage and maintaining a strict train-test split that properly assesses generalization to truly unseen procedurally generated scenarios. Following and extending the benchmark protocol from the latest work [21], we created a mixed-quality dataset with equal proportions (1/3 each) of expert, medium, and random trajectories. Expert trajectories were collected from fully-trained PPO agents [36], medium trajectories from agents achieving 50% of expert performance, and random trajectories from uniformly random action selection. Expert trajectories were collected from PPO agents trained until convergence (when learning plateaued) rather than for a fixed number of steps, ensuring optimal performance for each game's unique characteristics. This mixed composition introduces additional challenges compared to standard offline RL benchmark [21] by reducing the proportion of successful episodes. The dataset is stored in standard (s, a, r, s') format where observations s are 64×64×3 RGB images, actions a vary by environment-specific action spaces, and rewards are sparse—appearing only at episode termination in all five selected environments. This extreme sparsity in reward signals presents a particularly challenging scenario for world model learning, as the model must learn long-horizon dynamics without intermediate reward guidance. The hyperparameters of behavior policy are provided at Appendix F.

E Analysis

E.1 Emergent Curriculum Effect

Our results demonstrate a clear emergent curriculum effect through the Prioritized Level Replay mechanism. As shown in Figure 2, the PLR approach initially selects similar episode lengths to random sampling while achieving higher returns. However, after approximately 4M training steps, a significant shift occurs where PLR begins prioritizing substantially longer episodes (up to $2.4 \times$ longer in some environments) while temporarily accepting lower comparative returns. This behavior indicates that the autocurriculum naturally discovers and focuses on more challenging, temporally-extended scenarios as the agent's capabilities improve, without requiring any manual curriculum design or environment-specific knowledge.

E.2 Component Contributions

The ablation study in Table 2 reveals the critical importance of combining both PLR and random horizon sampling. While fixed-horizon world models show reasonable performance (e.g., 3.71 on Jumper), incorporating random horizons improves results by 11% (4.11), and adding PLR-based prioritization yields an additional 41% improvement (5.78). This suggests that the success of IMAC stems from the synergistic effect of (1) diverse training experiences through random horizons preventing overfitting to fixed-length dynamics, and (2) intelligent prioritization that focuses computational resources on the most informative imagined trajectories.

E.3 Generalization Mechanisms

The superior generalization of IMAC can be attributed to its ability to generate and prioritize diverse imagined experiences beyond the offline dataset distribution. By training exclusively on imagined rollouts from a world model learned on 200 levels, our agents achieve strong performance on unseen test levels (201+), with improvements ranging from 17% to 48% over model-free baselines. This suggests that the combination of world models and autocurricula enables agents to explore a richer space of potential scenarios than what exists in the original offline data, effectively augmenting the training distribution in a principled manner.

F Baseline Algorithm Hyperparameters

We conducted comprehensive hyperparameter optimization for all baseline algorithms using grid search following the previous benchmark work [21]. All model-free offline RL methods (BCQ, CQL, IQL) and behavior cloning (BC) shared identical encoder architectures, utilizing ResNet for visual feature extraction from the 64×64×3 Procgen observations. Experiments were executed on NVIDIA RTX 4090 GPUs with 24GB memory. For behavior cloning (BC), we explored batch sizes $\in \{64, 128, 256, 512\} \text{ and learning rates} \in \{5 \times 10^{-3}, 1 \times 10^{-4}, 5 \times 10^{-4}, 6 \times 10^{-5}\}. \text{ The Q-learning rates} \in \{5 \times 10^{-3}, 1 \times 10^{-4}, 5 \times 10^{-4}, 6 \times 10^{-5}\}.$ based methods (BCQ, CQL, IQL) employed dual-network architectures with target networks, where we investigated both Polyak averaging and direct weight copying strategies. For direct copying, we tested update frequencies $\{1,100,1000\}$, while for Polyak averaging, we examined $\tau \in$ {0.005, 0.5, 0.99}. Algorithm-specific hyperparameters included: BCQ's action selection threshold $\in \{0.3, 0.5, 0.7\}$; CQL's regularization coefficient $\alpha \in \{0.5, 1.0, 4.0, 8.0\}$; and IQL's temperature $\in \{3.0, 7.0, 10.0\}$ with expectile weights $\in \{0.7, 0.8, 0.9\}$. For sequence modeling approaches (DT, BCT), we additionally optimized context lengths $\in \{5, 10, 30, 50\}$. Decision Transformer utilized return-to-go multipliers $\in \{1,5\}$, where the maximum return was determined from training data and scaled accordingly. Both DT and BCT maintained a dropout rate of 0.1 following [44]. Table 5 presents the final selected hyperparameters achieving optimal performance on our 1M-step mixed dataset.

Table 5: Final hyperparameter configurations for baseline algorithms on 1M mixed dataset

Algorithm	Hyperparameter	Value	
BC	Learning Rate	0.0005	
ьс	Batch Size	256	
	Learning Rate	0.0005	
ВСТ	Batch Size	512	
вст	Context Length	30	
	Eval Return Multiplier	0	
	Learning Rate	0.0005	
DT	Batch Size	512	
DI	Context Length	10	
	Eval Return Multiplier	5	
	Learning Rate	0.0005	
BCQ	Batch Size	256	
ьсу	Target Model Weight Update	Direct copy	
	au	-	
	Target Update Frequency		
	Threshold	0.5	
	Learning Rate	0.0005	
	Batch Size	256	
CQL	Target Model Weight Update	Direct copy	
	au	-	
	Target Update Frequency	1000	
	Alpha	4.0	
	Learning Rate	0.0005	
	Target Model Weight Update	Direct copy	
IQL	Batch Size	512	
.45	au	-	
	Target Update Frequency	100	
	Temperature	3.0	
	Expectile	0.8	

G Training Time Profile

Table 6 presents a comprehensive breakdown of computational time requirements for training IMAC 1 game per seed.

Table 6: Detailed computational time analysis for IMAC training pipeline. Measurements were obtained using an NVIDIA RTX 4090 GPU with hyperparameters detailed in previous sections. These timing results serve as representative benchmarks, with actual runtimes varying based on hardware configuration, environment setup, and specific training conditions.

Component	Time (hours)			
World Model Training (Offline)				
Diffusion model	6.8			
Reward/Termination model	5.4			
Agent Training				
Total (1000 epochs)	75.0			
Per epoch (avg)	0.075			
Total Training Time	87.2			